Flow in BEC past an obstacle

Gennady A. El[1], Arnaldo Gammal[2],
Anatoly M. Kamchatnov[3]

[1]Loughborough University, UK
[2]Universidade de São Paulo, São Paulo, Brazil
[3]Institute of Spectrocopy, Russian Academy of Science

Estudantes do IFUSP envolvidos

Eduardo Georges Khamis

Éder Santana Annibale

-Classical fluid past obstacles
-BEC past obstacles
-Kelvin ship waves
-Oblique dark solitons
-Nonlinear Optics “Hydrodinamics”

Classical Fluids with viscosity

$$\frac{\partial \rho}{\partial t} + \nabla(\rho \mathbf{v}) = 0$$ continuity

$$\frac{\partial \mathbf{v}}{\partial t} + (\mathbf{v}.\nabla)\mathbf{v} = -\frac{1}{\rho}\left\{\nabla p + \eta \nabla^2 \mathbf{v} + \left(\zeta + \frac{\eta}{3}\right)\nabla(\nabla.\mathbf{v})\right\}$$

momentum conservation

Navier(1827) & Stokes (1845)
with viscosity η
2nd viscosity ζ

Viscous imcompressible homogeneous fluid

No. de Reynolds

$$\mathrm{Re} = D v_0 \rho / \eta$$

Similarity principle of Reynolds (1883)

D = depends of the shape/size of the body [L]
v_0 = flux velocity

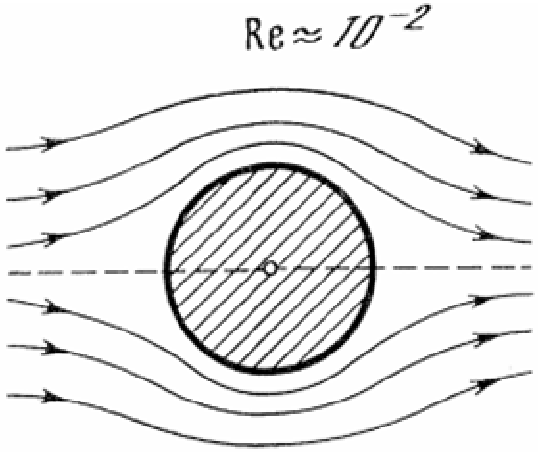

Fig. 9.1. Laminar flow around a cylinder for small Re

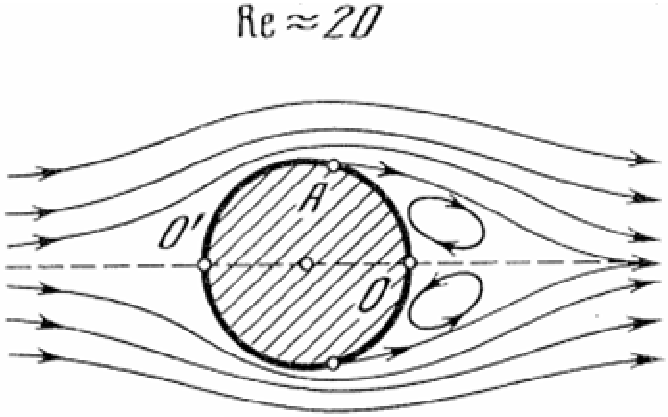

Fig. 9.2. Steady flow past a cylinder with two vortices

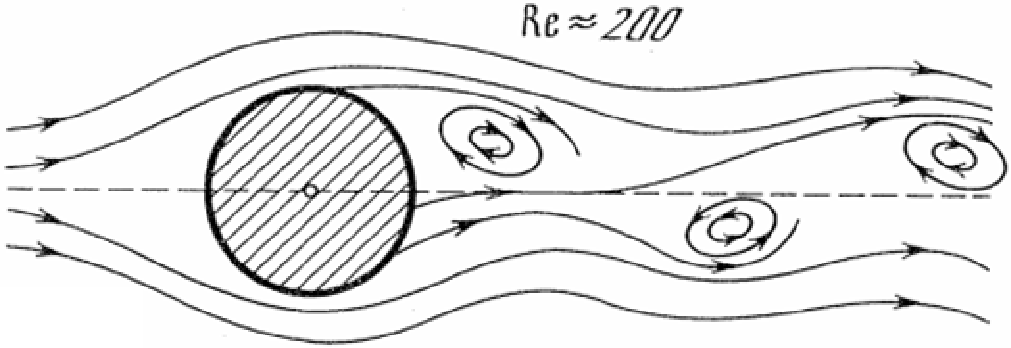

Fig. 9.3. Illustrating a Karman street

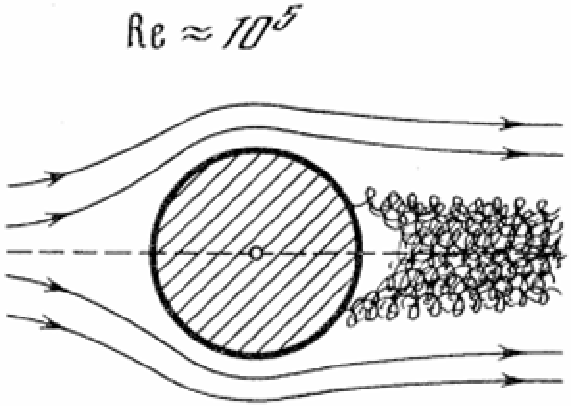

Fig. 9.4. The flow with a fully developed turbulent wake

1.3-kilometer high volcanic island of Guadalupe, west of Baja California in the Pacific Ocean.
 was taken by the Multi-angle Imaging SpectroRadiometer (MISR) camera

Vortices behind a cylinder

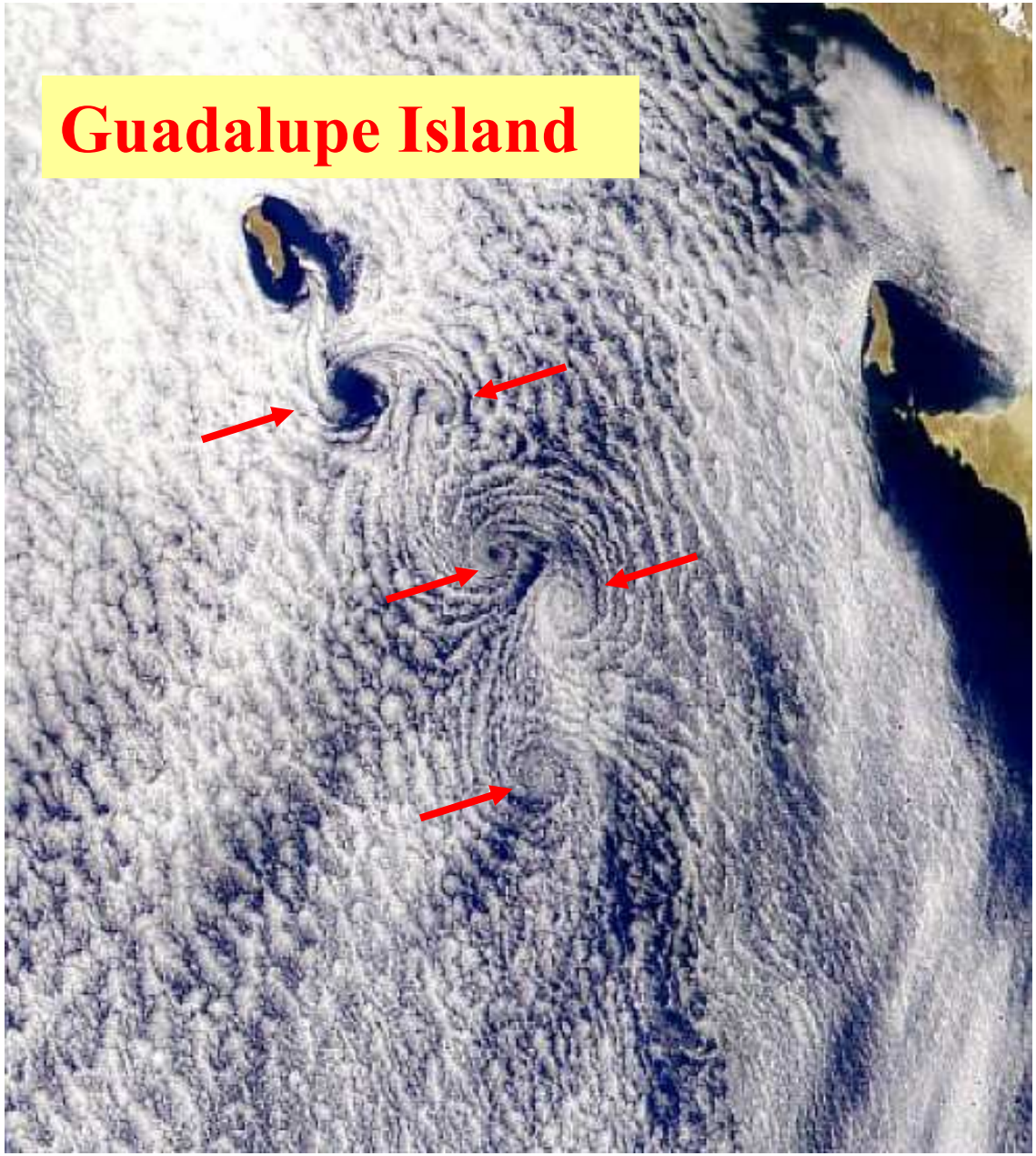

"Von- Karman vortex street"

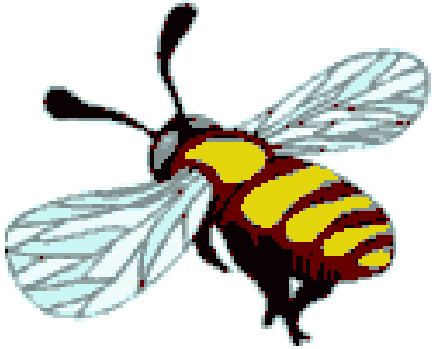

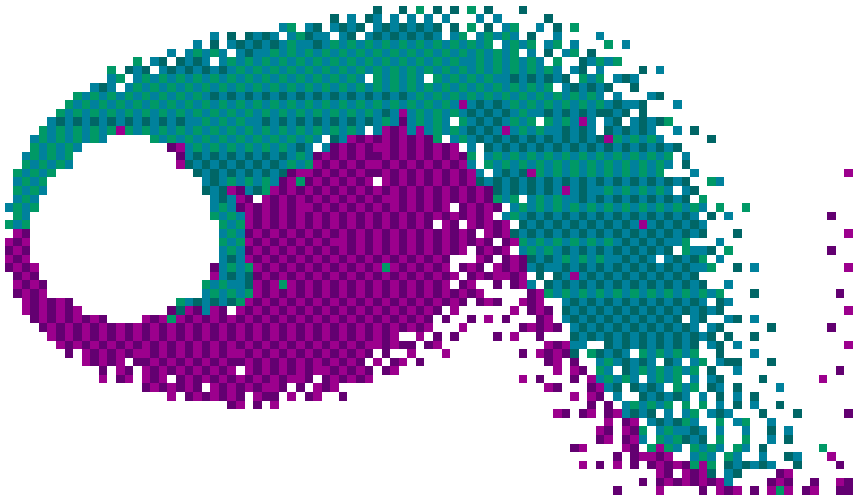

Classical supersonic flow, M=1.5

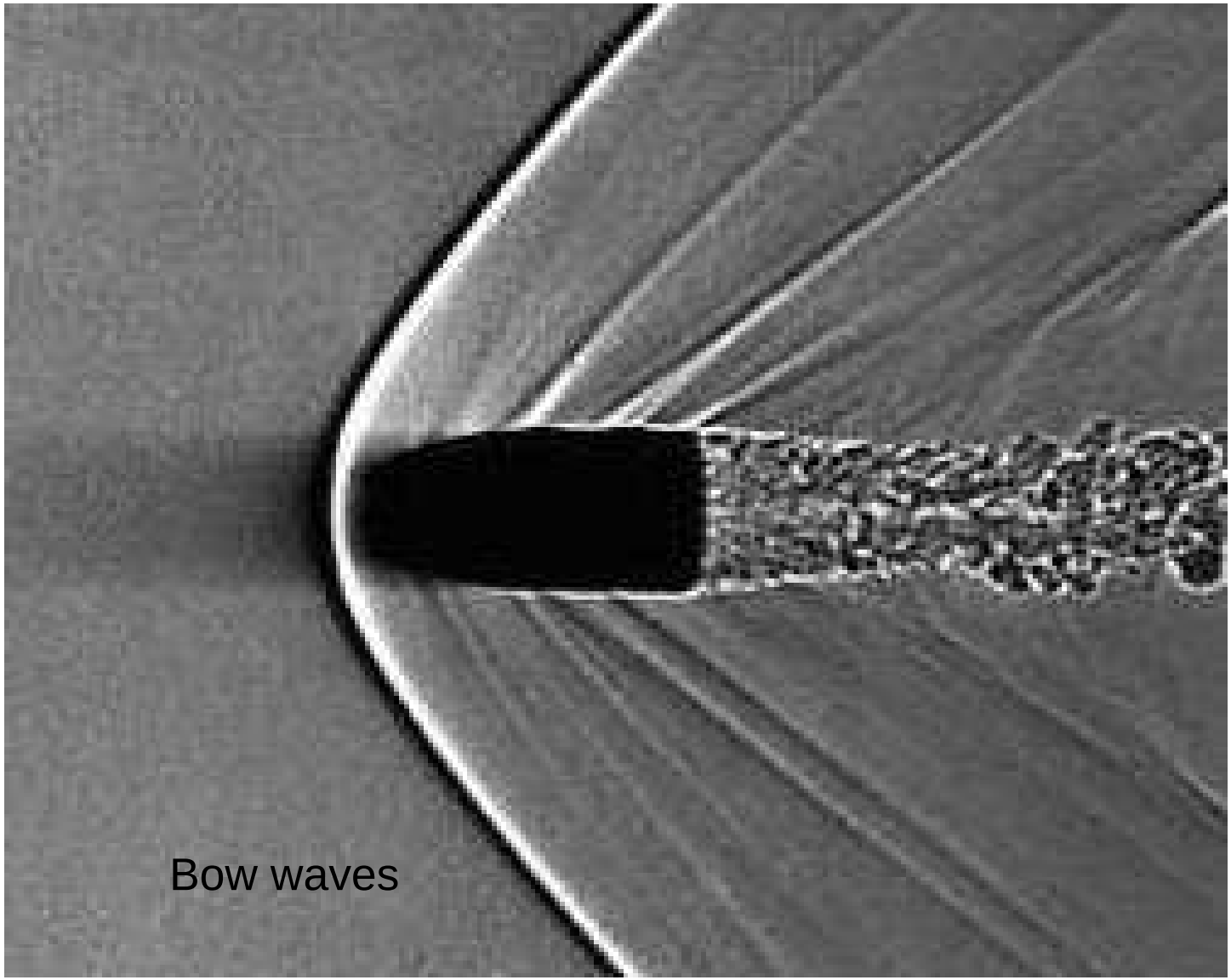

by Andrew Davidhazy
Rochester Institute of Technology

Quantum Fluids- BEC

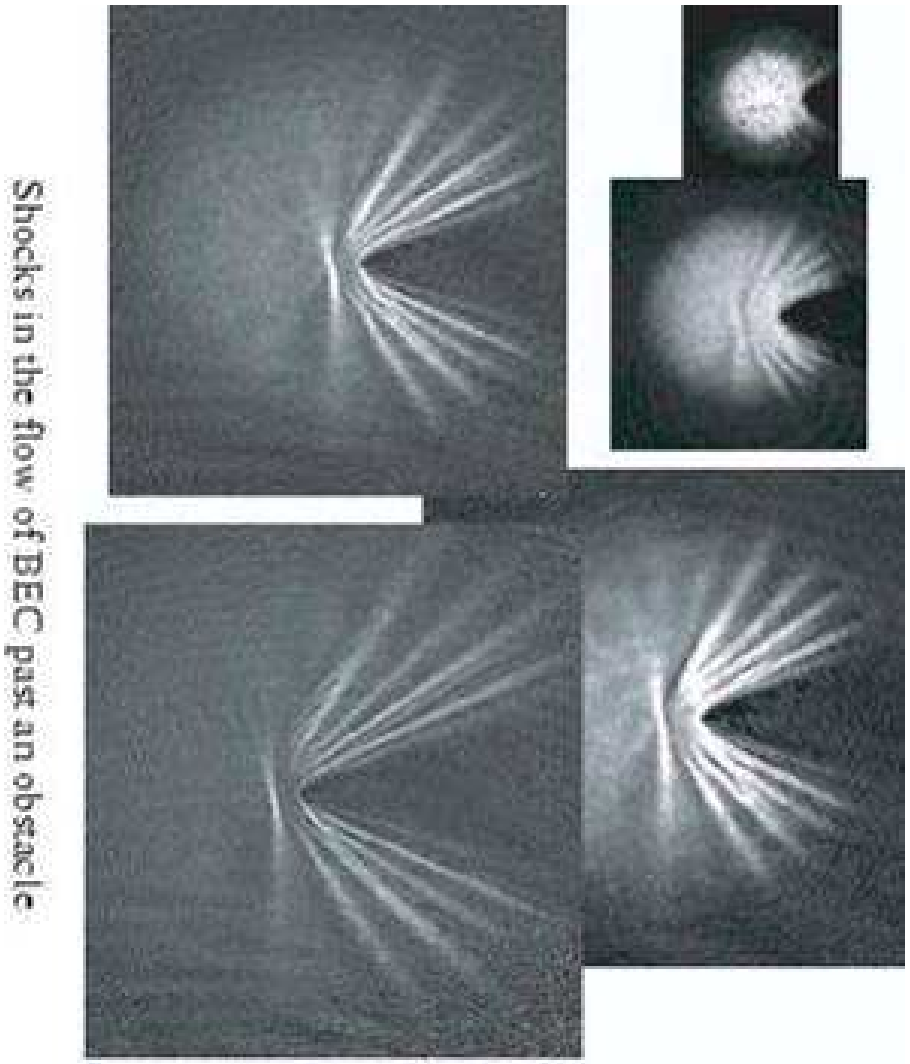

JILA 2005

the source
ed in this
es emitted
by a strong
,7], to the
supersonic
[8], and in
by a boat
Letter we
erturbation
hich flows
perimental
a Galilean
e in a sta-
of a uni-
stationary
y letting a
localized

the BEC density profile after different expansion times t_{exp} are then taken by means of destructive absorption imaging. Two examples are shown in Fig. 1. The field of view is centered in the region around the defect in order to observe

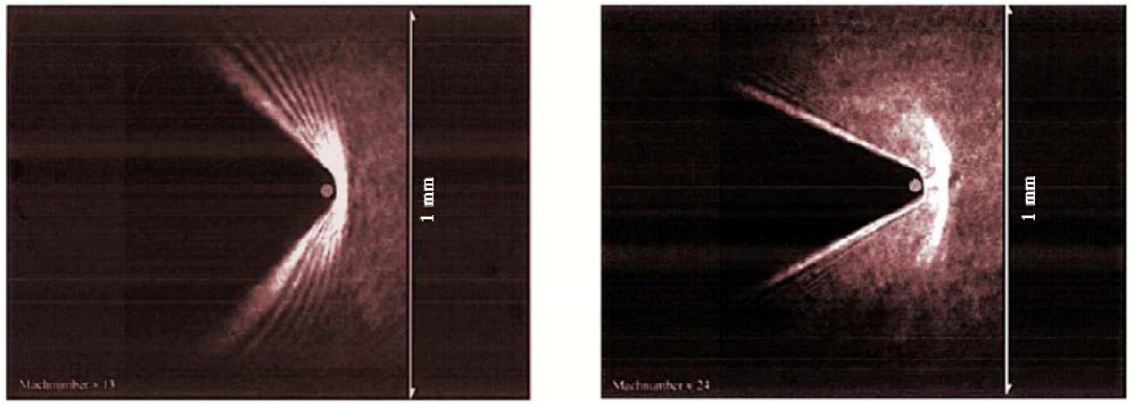

FIG. 1 (color online). Experimental [10] density profiles (integrated along z) of a BEC hitting an obstacle at supersonic velocities $v/c_s = 13$ (a) and 24 (b). The angles of the conical wave fronts are $\sin(\theta) = 0.73$ and $\sin(\theta) = 0.43$, respectively. The condensate flow is from the right to the left.

JILA

Carusotto et.al, PRL(2006)

Gross-Pitaevskii equation

Dynamics of a dilute condensate is described by the Gross-Pitaevskii equation

$$i\hbar\frac{\partial\psi}{\partial t}=-\frac{\hbar^2}{2m}\Delta\psi+V_{ext}(\mathrm{r})\psi+g\,|\psi|^2\,\psi$$

where

$$V_{ext}(\mathrm{r})=\frac{m}{2}(\omega_x^2x^2+\omega_y^2y^2+\omega_z^2z^2)$$

$$g = \frac{4\pi\hbar^2 a_s}{m},$$

a_s is the atom-atom scattering length,

$\int |\psi|^2 \, d\mathbf{r} = N,$ N is number of atoms in the trap.

$$l_0 = \sqrt{\frac{\hbar}{m\omega}}$$

Disc-shaped trap

$$\lambda = \frac{\omega_z}{\omega_\perp} >> 1, \qquad \psi(\mathrm{r},t) = \phi(z)\Psi(x,y,t),$$

$$\phi(z) = \frac{1}{\pi^{1/4} a_z^{1/2}} \exp(-\frac{z^2}{2a_z^2}),$$

$$i\hbar \frac{\partial \Psi}{\partial t} = -\frac{\hbar^2}{2m}\Delta_\perp \Psi + \frac{1}{2} m(\omega_x^2 x^2 + \omega_y^2 y^2)\Psi + g_{2D} |\Psi|^2 \Psi$$

$$g_{2D} = \frac{g}{\sqrt{2\pi} a_z} = \frac{2\sqrt{2\pi}\hbar^2 a_s}{m a_z}, \qquad \int |\Psi|^2 \, dxdy = N.$$

Bose-Einstein Condensates-dimensionless units

$$i\frac{\partial \psi}{\partial t} = -\frac{1}{2}\nabla^2\psi + |\psi|^2\psi$$

$$\psi = \sqrt{\rho}e^{i\varphi}$$

Madelung Transformation (1929)!

$$\mathbf{v} = \nabla\varphi$$

Gross-Pitaevskii Eq. in hydrodinamic form

$$\frac{\partial \rho}{\partial t} + \nabla(\rho \mathbf{v}) = 0$$

$$\frac{\partial \mathbf{v}}{\partial t} + (\mathbf{v}.\nabla)\mathbf{v} + \nabla\rho + \nabla\left[\frac{(\nabla\rho)^2}{8\rho^2} - \frac{\nabla^2\rho}{4\rho}\right] = 0$$

And sound velocity for uniform solution is

$$c_s = \sqrt{\rho}$$

No viscosity
quantum pressure term

E. Cornell (2005)

From GP to quantum hydrodynamics

How similar is quantum shock to classical shock?
→ need a hydrodynamic description of the BEC.

BEC: Gross-Pitaevskii equation

$$i\hbar\frac{\partial}{\partial t}\psi(\vec{r},t)=\left(-\frac{\hbar^2}{2m}\Delta+V_{extern}+\frac{4\pi\hbar^2 a}{m}|\psi(\vec{r},t)|^2\right)\psi(\vec{r},t)$$

$$\psi=f(\vec{r})\cdot e^{i\phi(r)} \quad\Rightarrow\quad n=f^2 \qquad \vec{v}=\frac{\hbar}{m}\nabla\phi$$

Hydrodynamic equation for a BEC

$$m\left(\frac{\partial v}{\partial t}+\nabla\left(\frac{v^2}{2}\right)\right)=-\nabla gn-\nabla V_{extern}+\nabla\left(\frac{\hbar^2}{2m\sqrt{n}}\nabla^2\sqrt{n}\right)$$

& continuity equation: $\dfrac{\partial n}{\partial t}+\nabla\cdot(v\,n)=0$

E. Cornell (2005)

Quantum Reynolds Number

Is the quantum pressure important at all?

Classical case:

Viscoscity important when low Reynolds number Re.

$$\mathrm{Re} = \frac{\text{inertial force}}{\text{viscous force}} = \frac{\rho(\mathrm{v}\cdot\nabla)\mathrm{v}}{\eta\Delta\mathrm{v}} \approx \frac{\rho \mathrm{v} L}{\eta}$$

Quantum case:

Compare mean field to quantum pressure.

$$\mathrm{Re} = \frac{\text{meanfield}}{\text{quantum pressure}} = \frac{4\pi\hbar^2 \mathrm{a}/\mathrm{m}\cdot\mathrm{n}}{\frac{\hbar^2}{2\mathrm{m}}\frac{\nabla^2\sqrt{\mathrm{n}}}{\sqrt{\mathrm{n}}}} \approx L^2 \mathrm{a}\ \mathrm{n} \approx \frac{L^2}{\xi_{\mathrm{heal}}^2}$$

L: characteristic length, e.g. width of shock front

→ QP important when important lengthscale beomces on order of healing length! (e.g. after sufficient self-steepening).

Numerical simulations

Let the order parameter ψ satisfies the initial condition

$$\Psi(x,y)\,|_{t=0} = \exp(iMx)$$

That is the flow with Mach velocity *M* is switched on at the moment t=0. We suppose that the potential V(x,y) corresponds to interaction of the condensate with the obstacle which is modeled by impenetrable disc with radius *r* . Numerical solution given *M* yield the evolution of the condensate.

Numerical calculations were made in the stationary frame with respect to the obstacle after making frame transformations so as the obstacle remained at rest

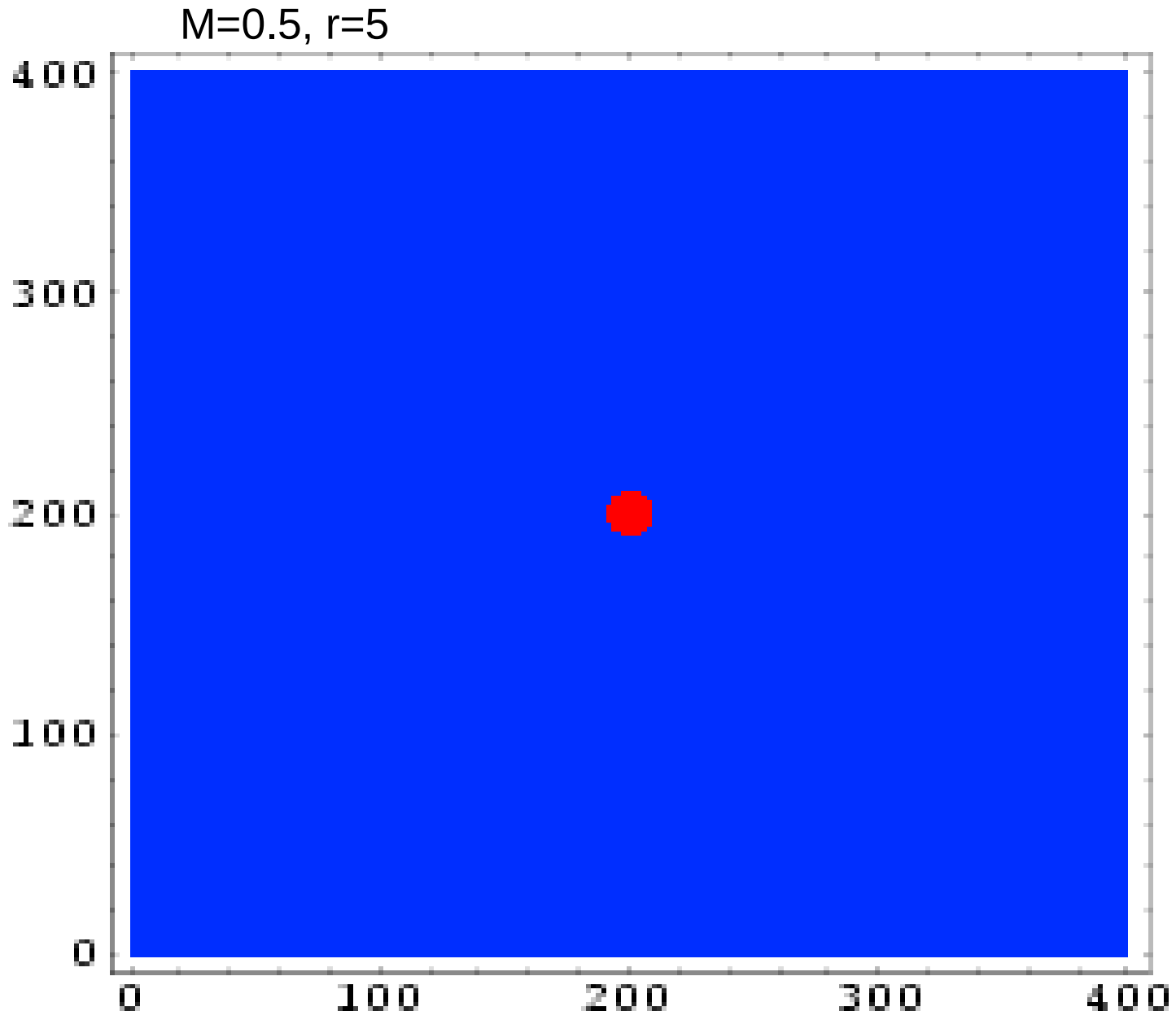

Low velocities -> vortex generation see Frisch et al PRL (1992)

M=0.5, r=5

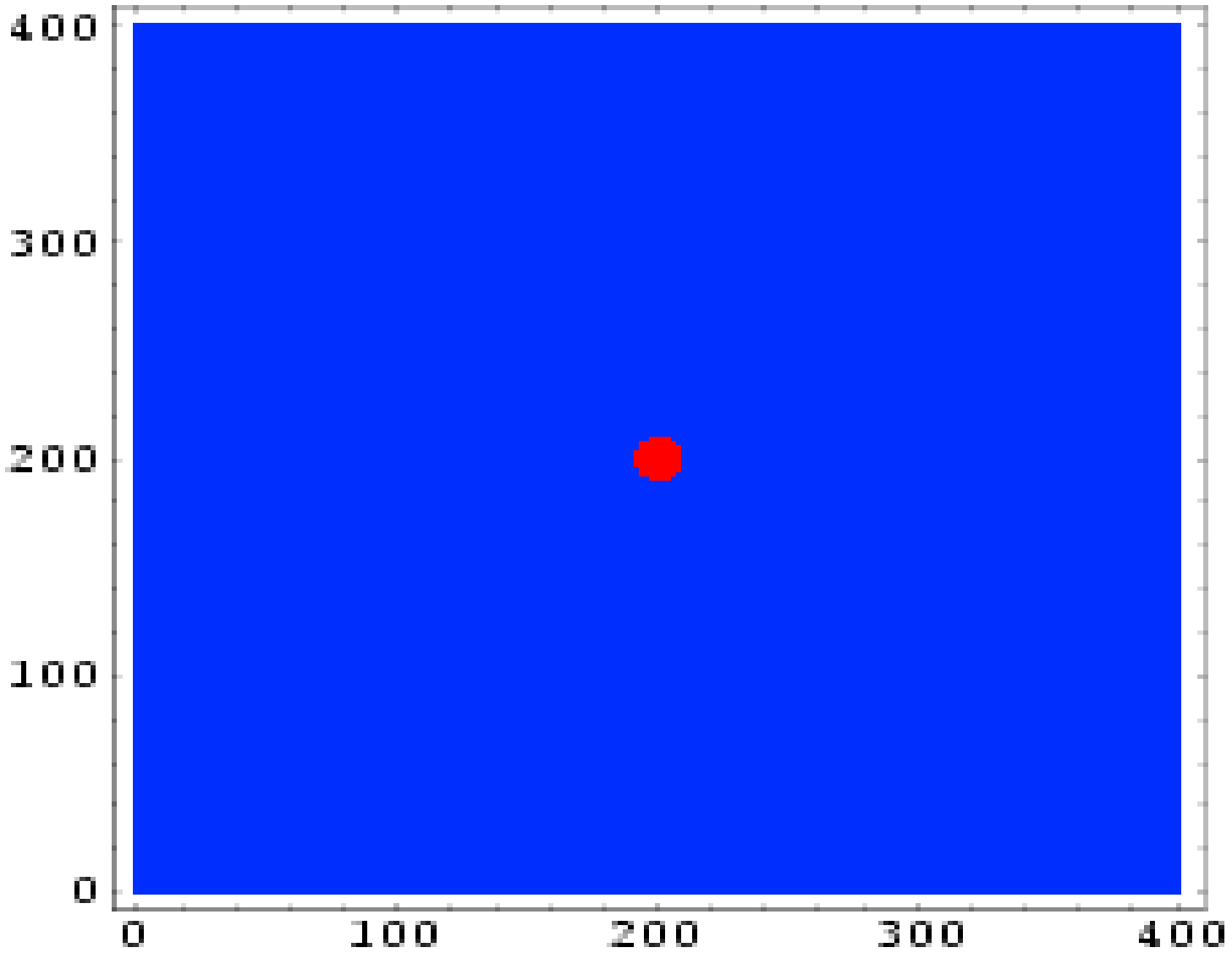

Low velocities -> vortex generation see Frisch et al PRL (1992)

M=0.5, r=5

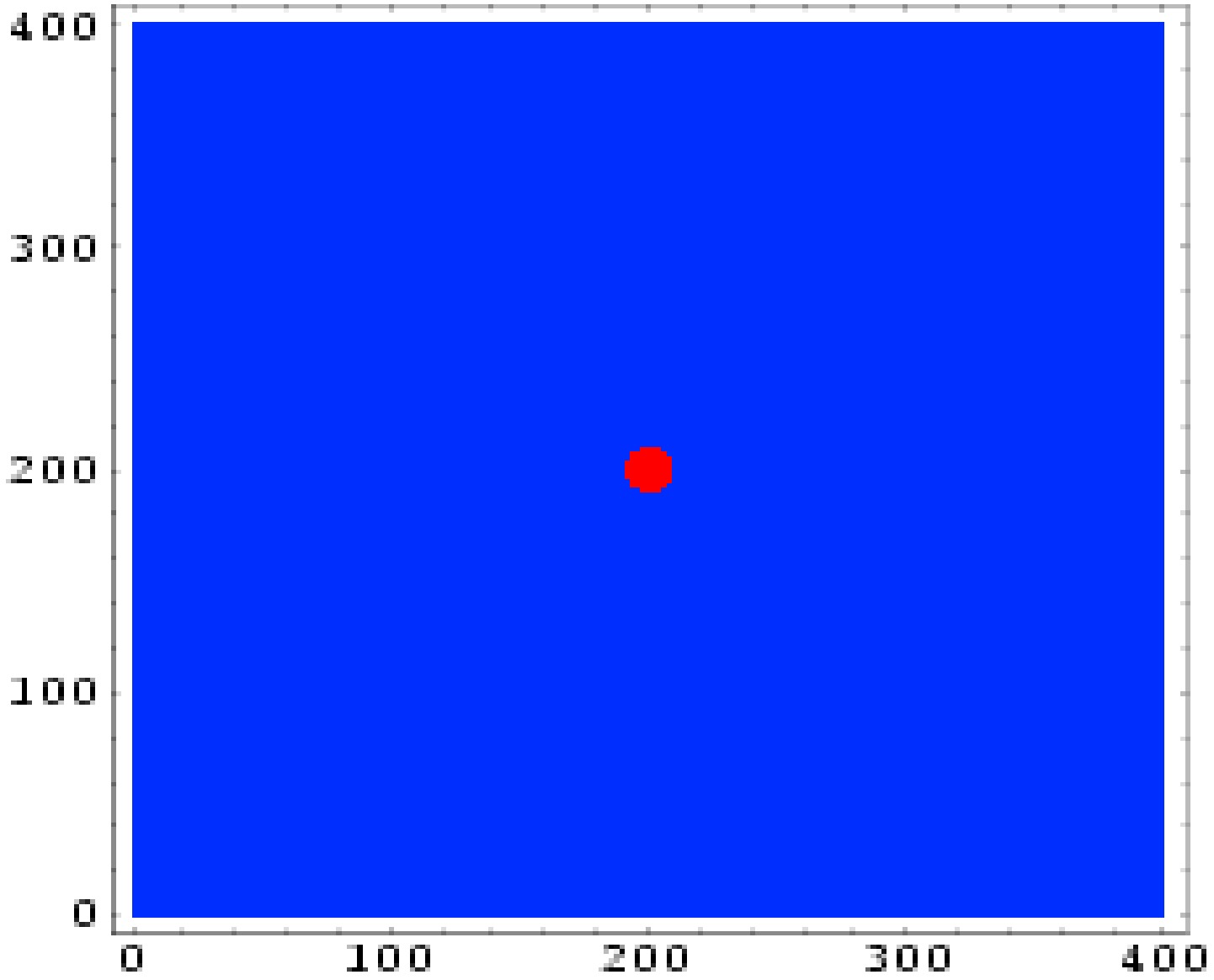

Low velocities -> vortex generation see Frisch et al PRL (1992)

Cornell (2005)

Vortices behind a small cylinder

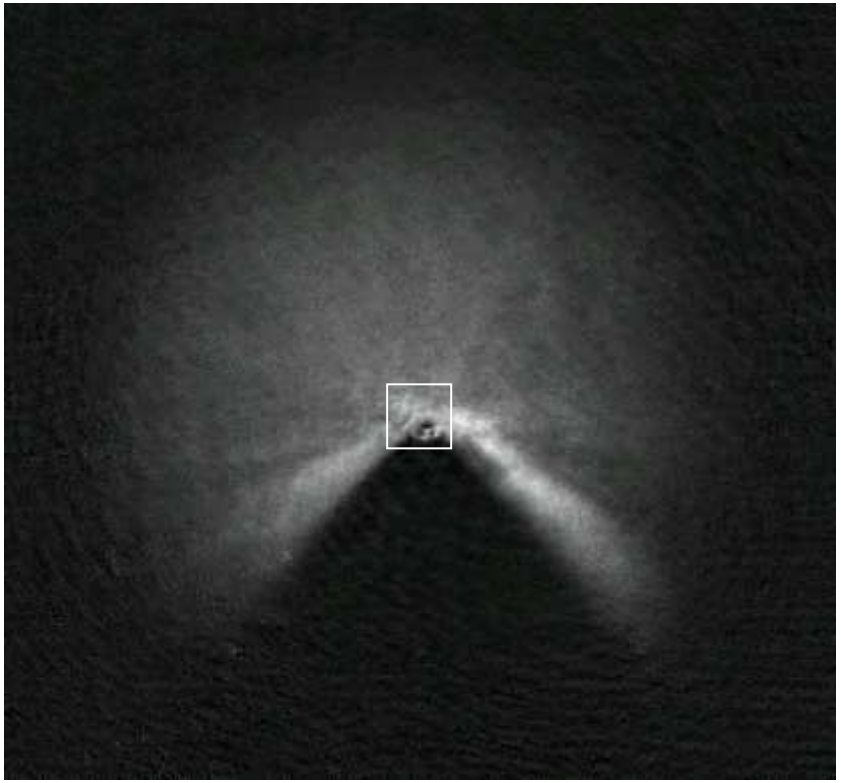

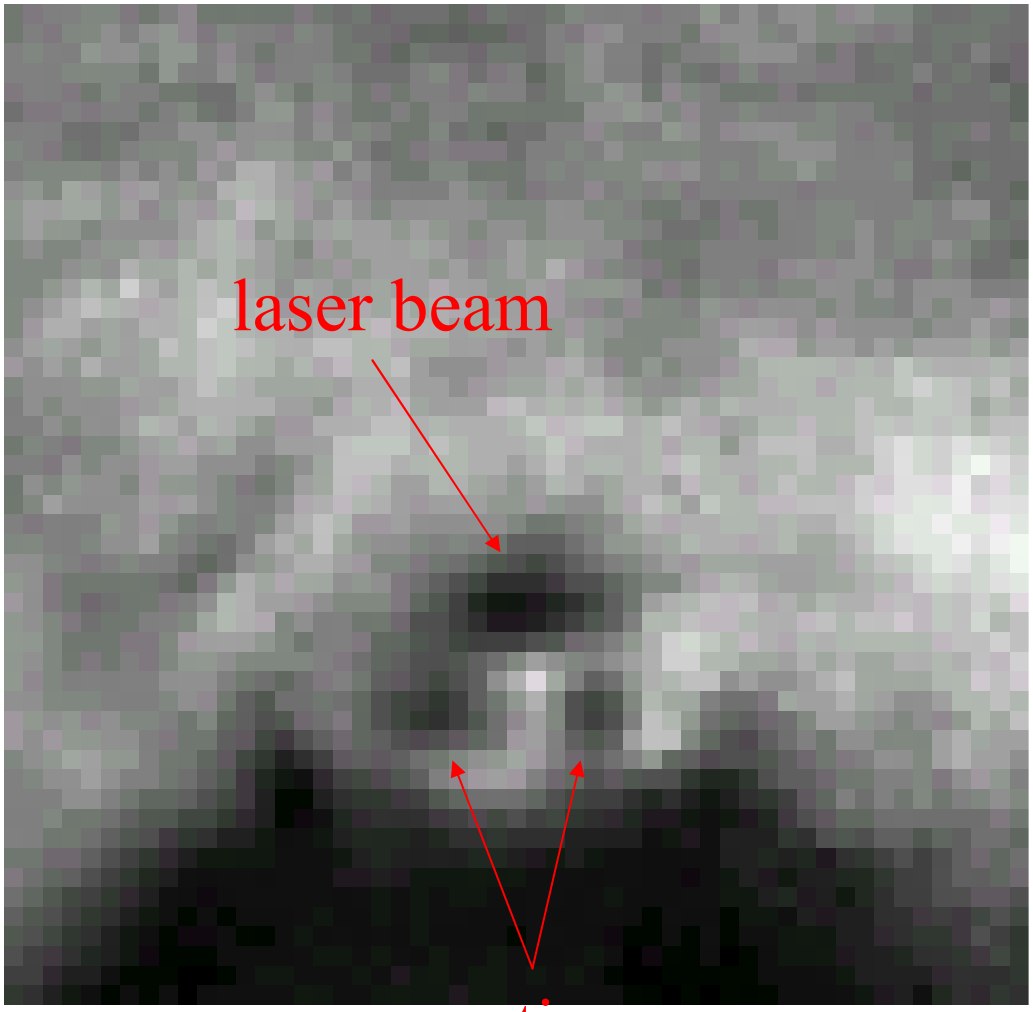

What happens
at supersonic flow M>1?

Winiecki, et 1999 reported vortex street…

M=5, r=1 Supersonic velocities

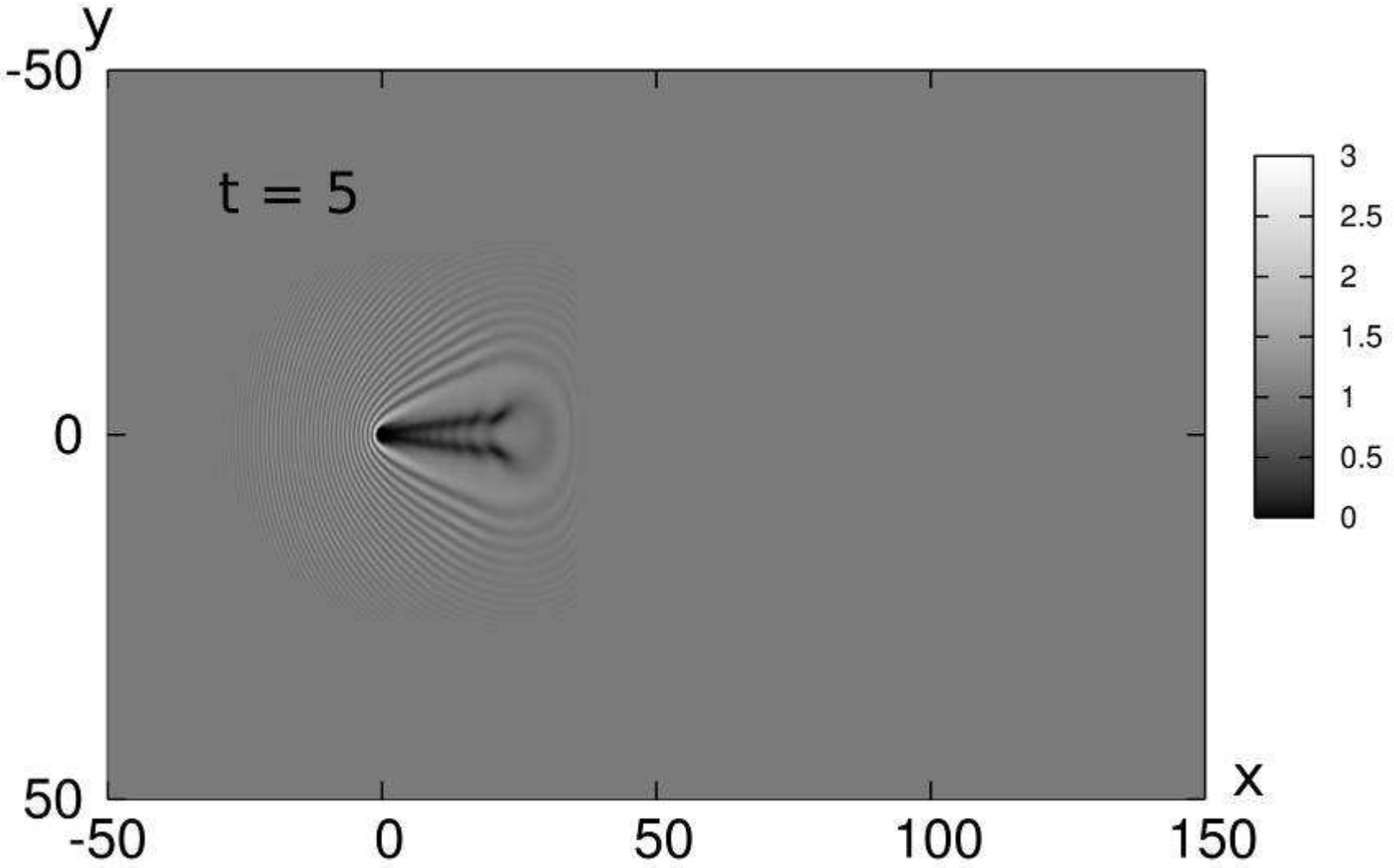

M=5, r=1

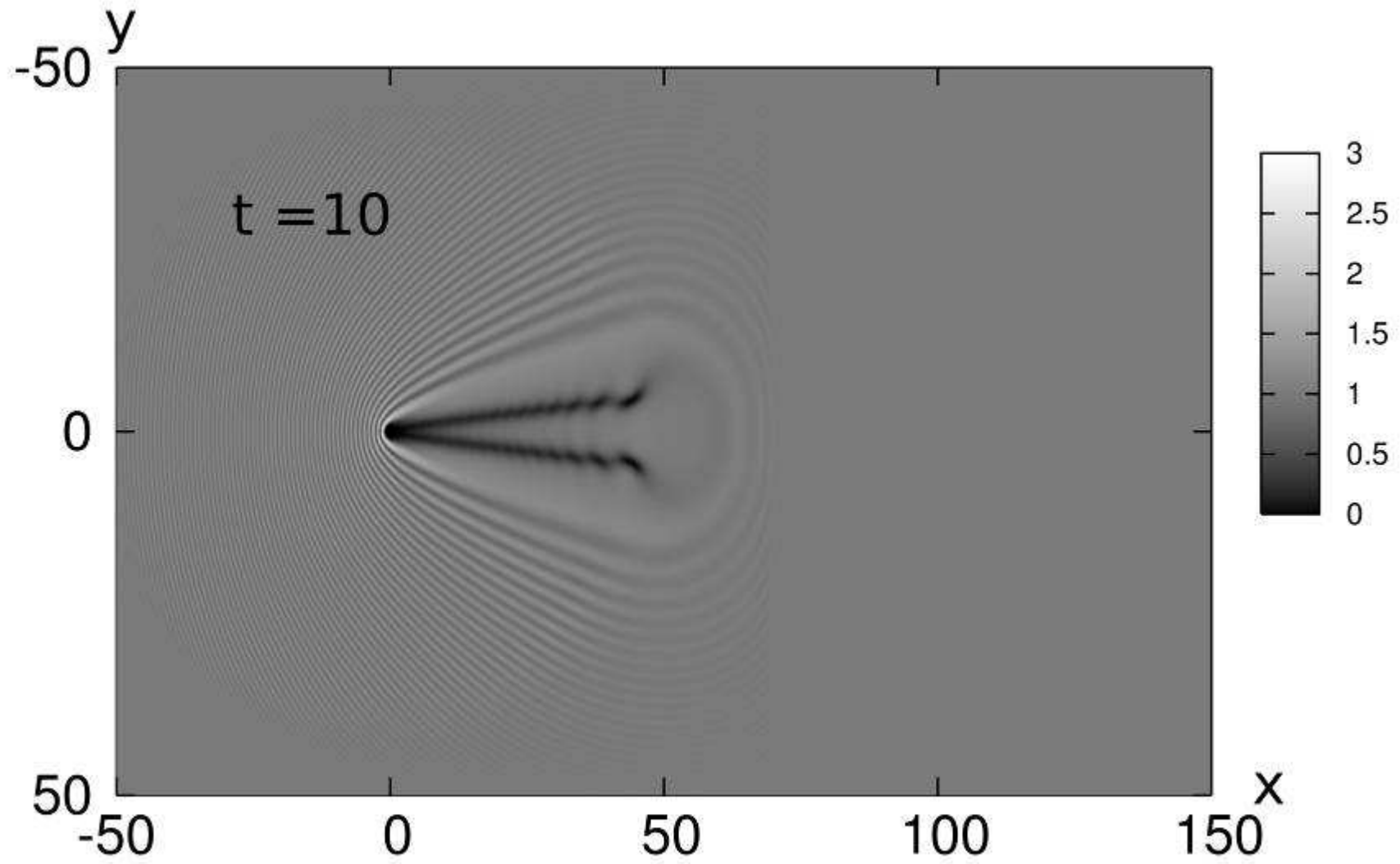

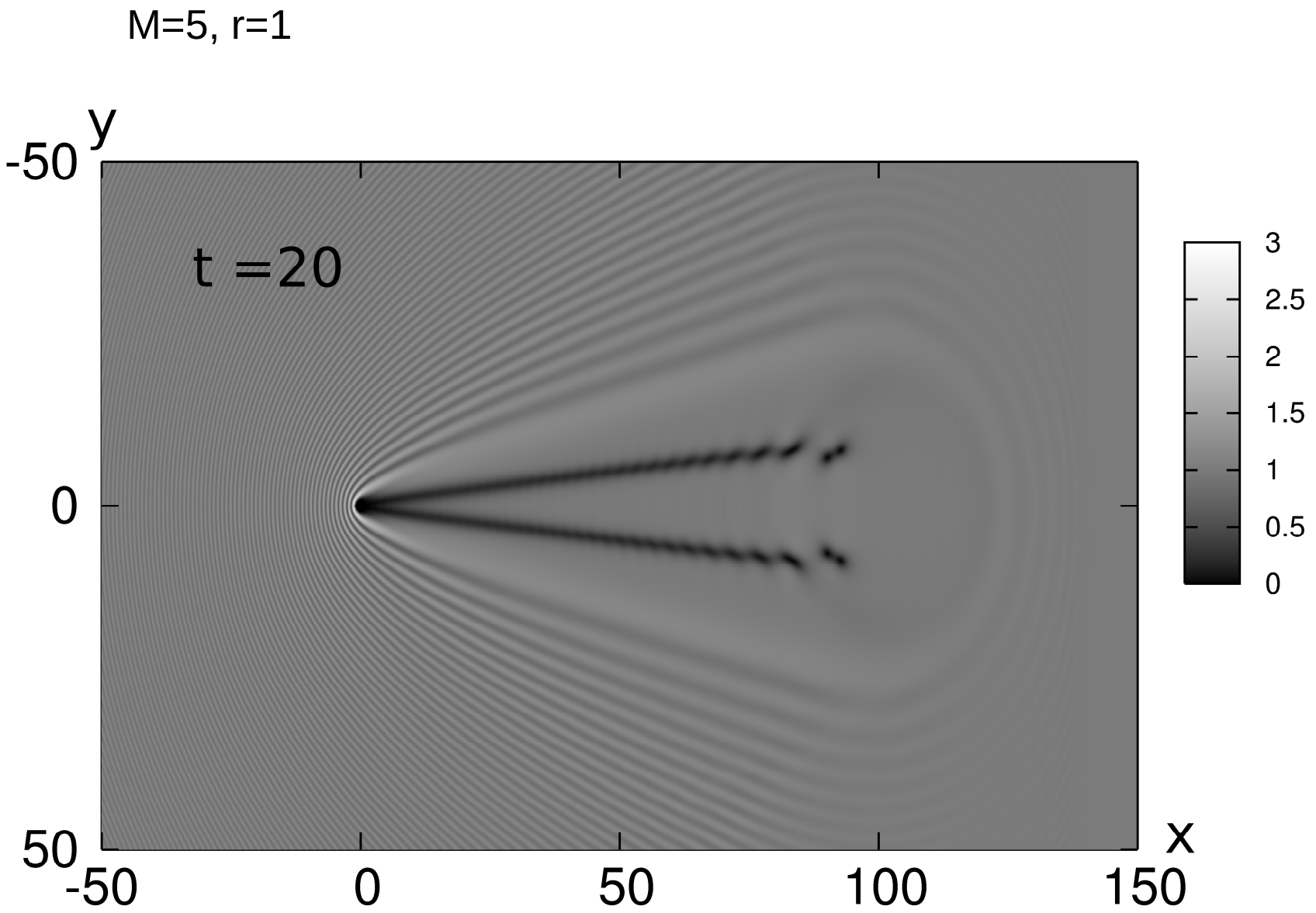
M=5, r=1
y
-50
t =20
0
50
x
-50
0
50
100
150
3
2.5
2
1.5
1
0.5
0

Now we consider in the hydrodynamic form a stationary system of equations for the density *n(x,y)* and two components of the velocity field **u**= *(u(x,y),v(x,y))*

$$(nu)_x + (nv)_y = 0$$

$$uu_x + vu_y + n_x + \left(\frac{n_x^2 + n_y^2}{8n^2} - \frac{n_{xx} + n_{yy}}{4n} \right)_x = 0$$

$$uv_x + vv_y + n_y + \left(\frac{n_x^2 + n_y^2}{8n^2} - \frac{n_{xx} + n_{yy}}{4n} \right)_y = 0$$

Far enough from the end points of the oblique soliton we can restrict our consideration to potential flows using the condition $u_y = v_x$.

Then the above equations can be integrated once to give

$$\frac{1}{2}\left(u^2 + v^2\right) + n + \frac{1}{8n^2}\left(n_x^2 + n_y^2\right) - \frac{1}{4}\left(n_{xx} + n_{yy}\right) = const$$

We look for the solution in the form

$$n = n(\theta), \qquad u = u(\theta), \qquad v = v(\theta), \qquad \text{where} \quad \theta = x - ay$$

and *a* denotes a slope of the soliton with respect to y axis.
It must also satisfy the boundary condition that BEC flow is uniform
At |*x*|-> *infinity n =1, u=M, v=0*

The velocity components can be easily expressed in terms of the density

$$u = \frac{M(1+a^2 n)}{(1+a^2)n}, \quad v = -\frac{aM(1-n)}{(1+a^2)n},$$

So that the system is reduced to the equation

$$\frac{1}{4}\left(1+a^2\right)\left(n_\theta^2 - 2nn_{\theta\theta}\right) + 2n^3 - (2+p)n^2 + p = 0,$$

where $$p = \frac{M^2}{1+a^2}$$

The above equation has the integral

$$\frac{1}{4}\left(1+a^2\right)n_\theta^2 = (1-n)^2(n-p)$$

Simple integration of this equation yields the soliton solution in the form

$$n(\theta) = 1 - \frac{1-p}{\cosh^2\left[\sqrt{1-p}\,\theta / \sqrt{1+a^2}\right]}$$

This formula give the exact dark spatial soliton solution of the 2D Gross-Pitaevskii equation. If the parameter *a* is determined from a numerically found slope of the oblique soliton then $n(\theta)$ describes the profile of the density of the condensate.

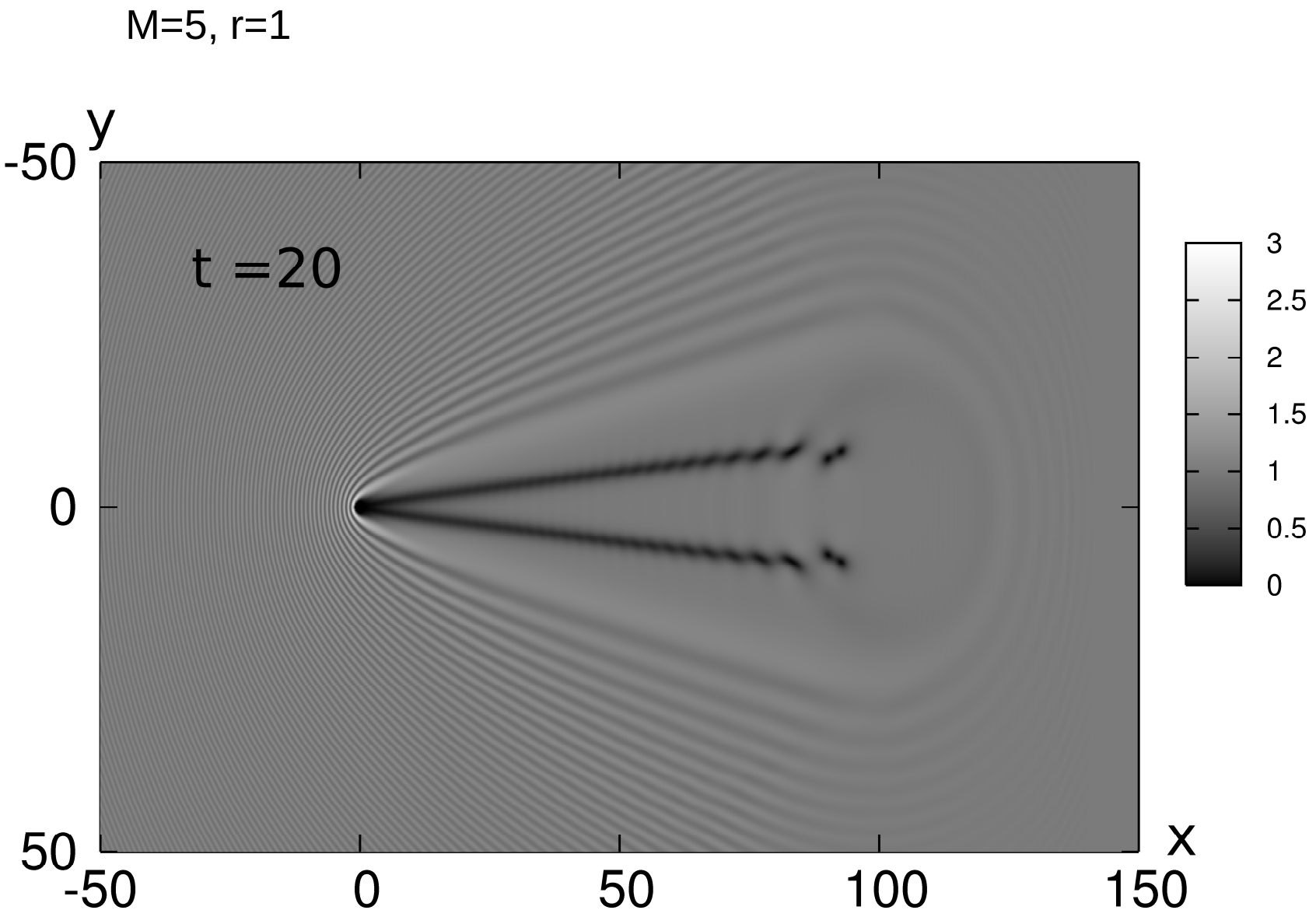

Cutting in x we see dark solitons

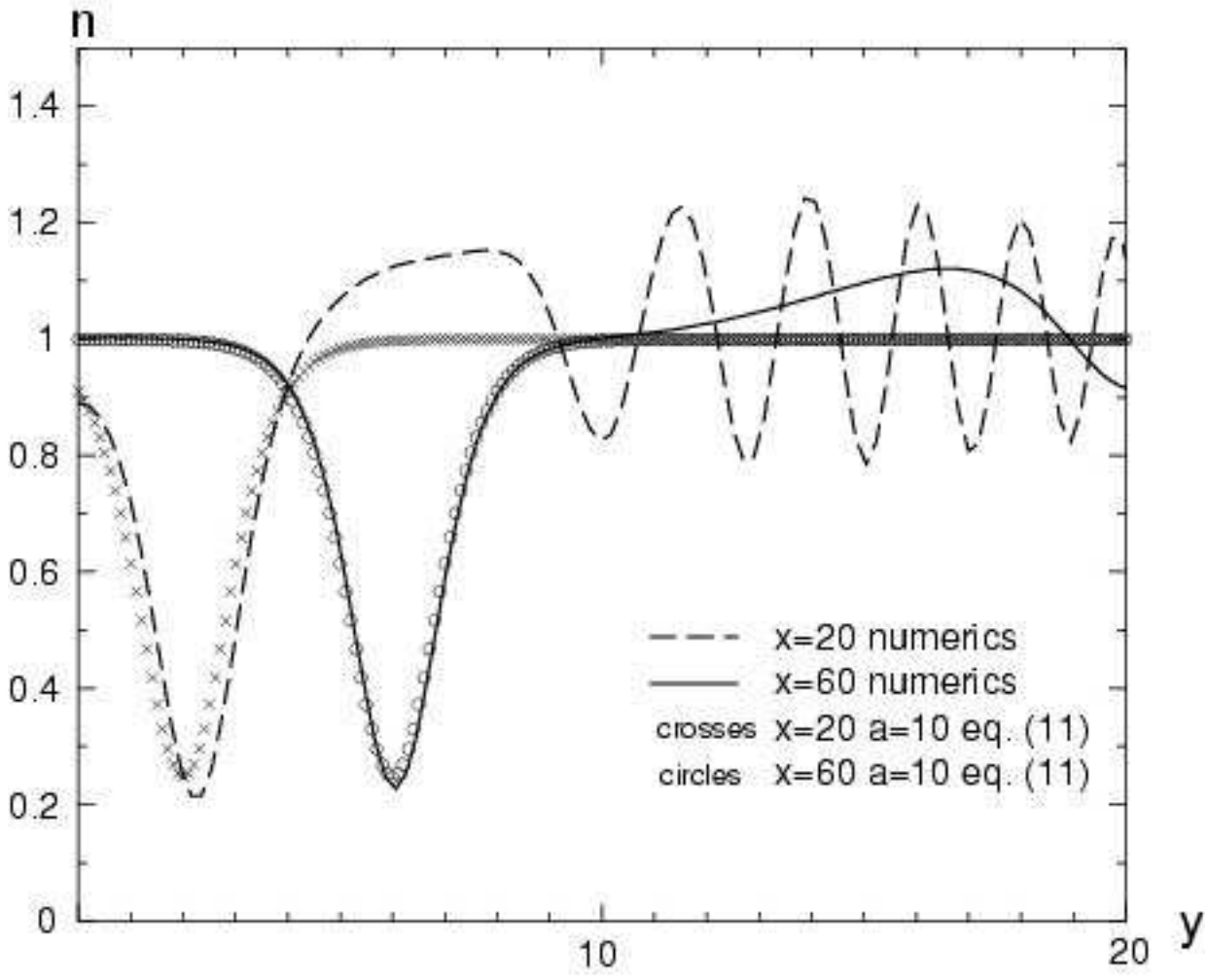

G.El, A.G., A.M.Kamchatnov
PRL (2006)

Differently from Navier-Stokes, that predicts turbulence for sufficient high velocities,
the potential flow in GP-2D at simple case showed to be *integrable*, which seems a remarkable result!

Increasing the radius -> more solitons!

M=5, r=5

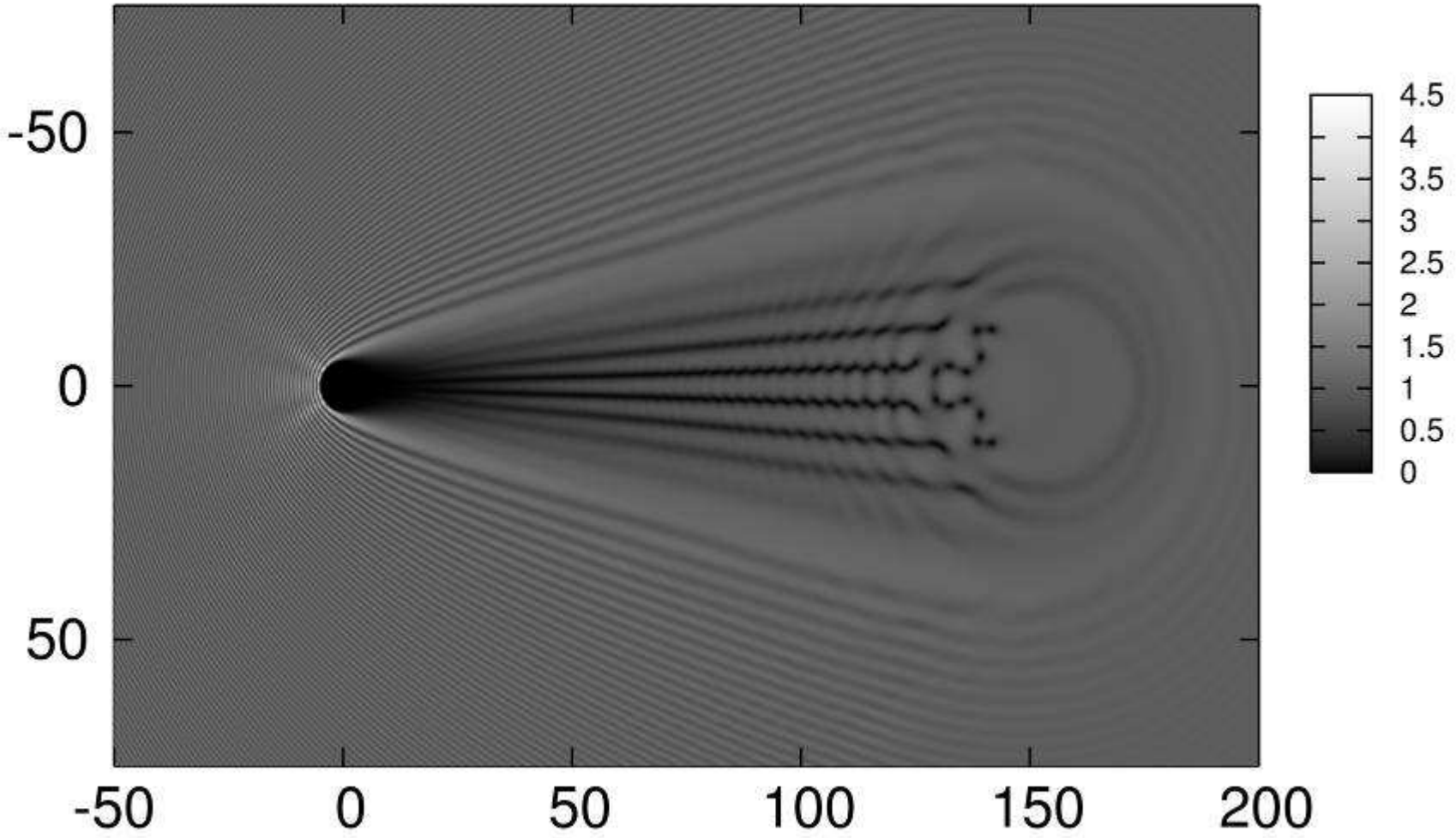

Increasing radius generate more dark solitons!

Kelvin
Ship waves

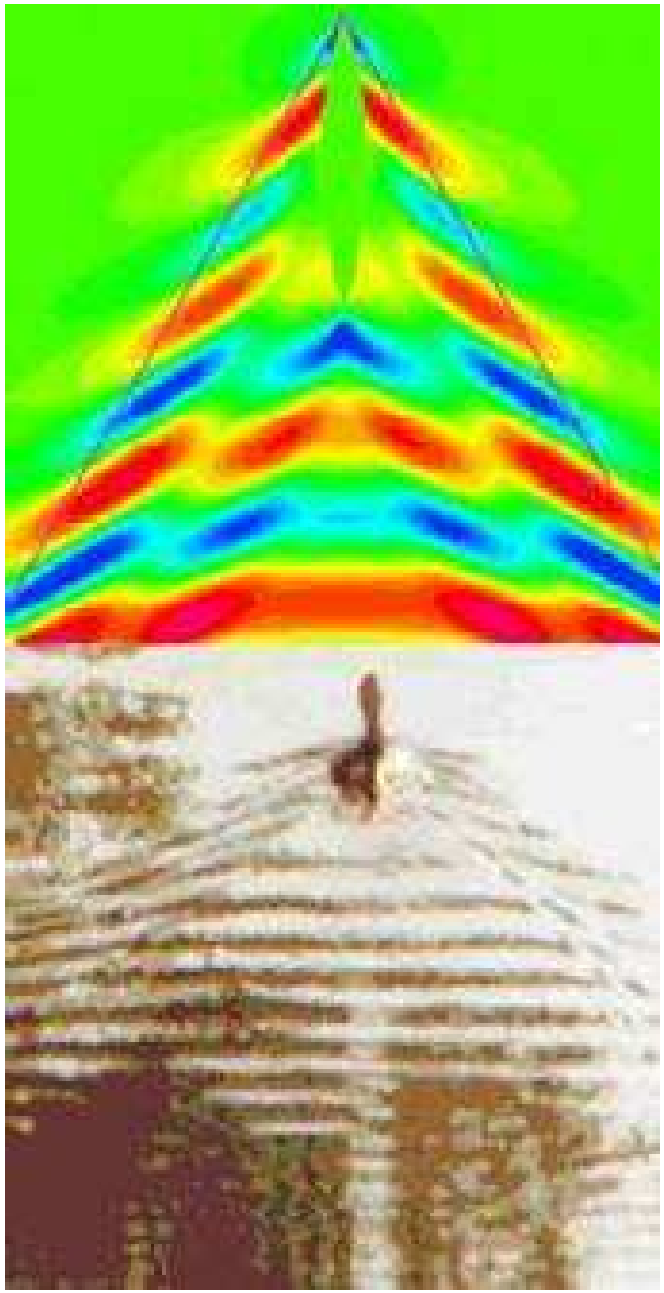

r=1, M=2

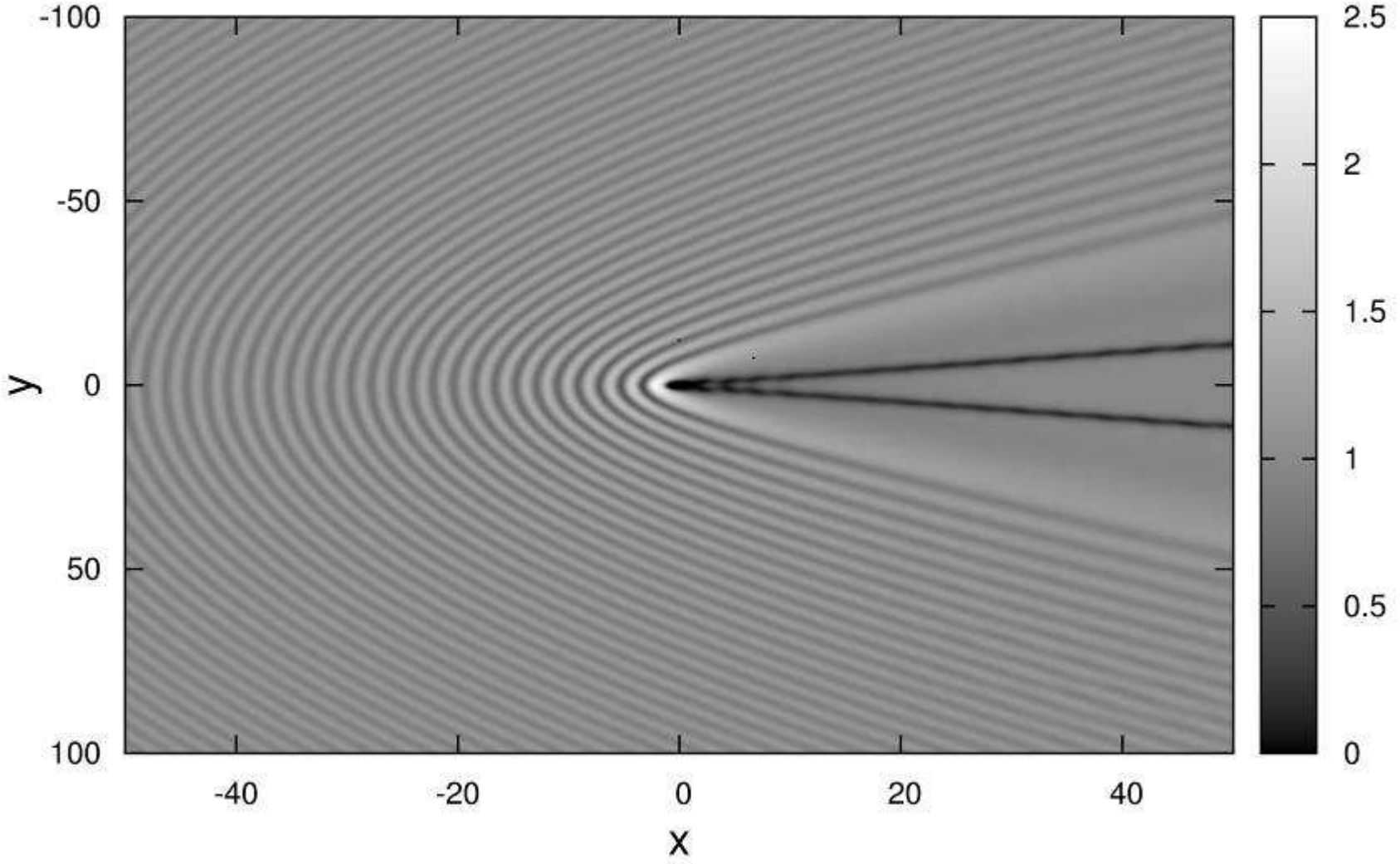

Using the same techniques developed by by Lord Kelvin applied to the GP equation were able to derive analytical shape of the “Ship waves” profile

r=1, M=2

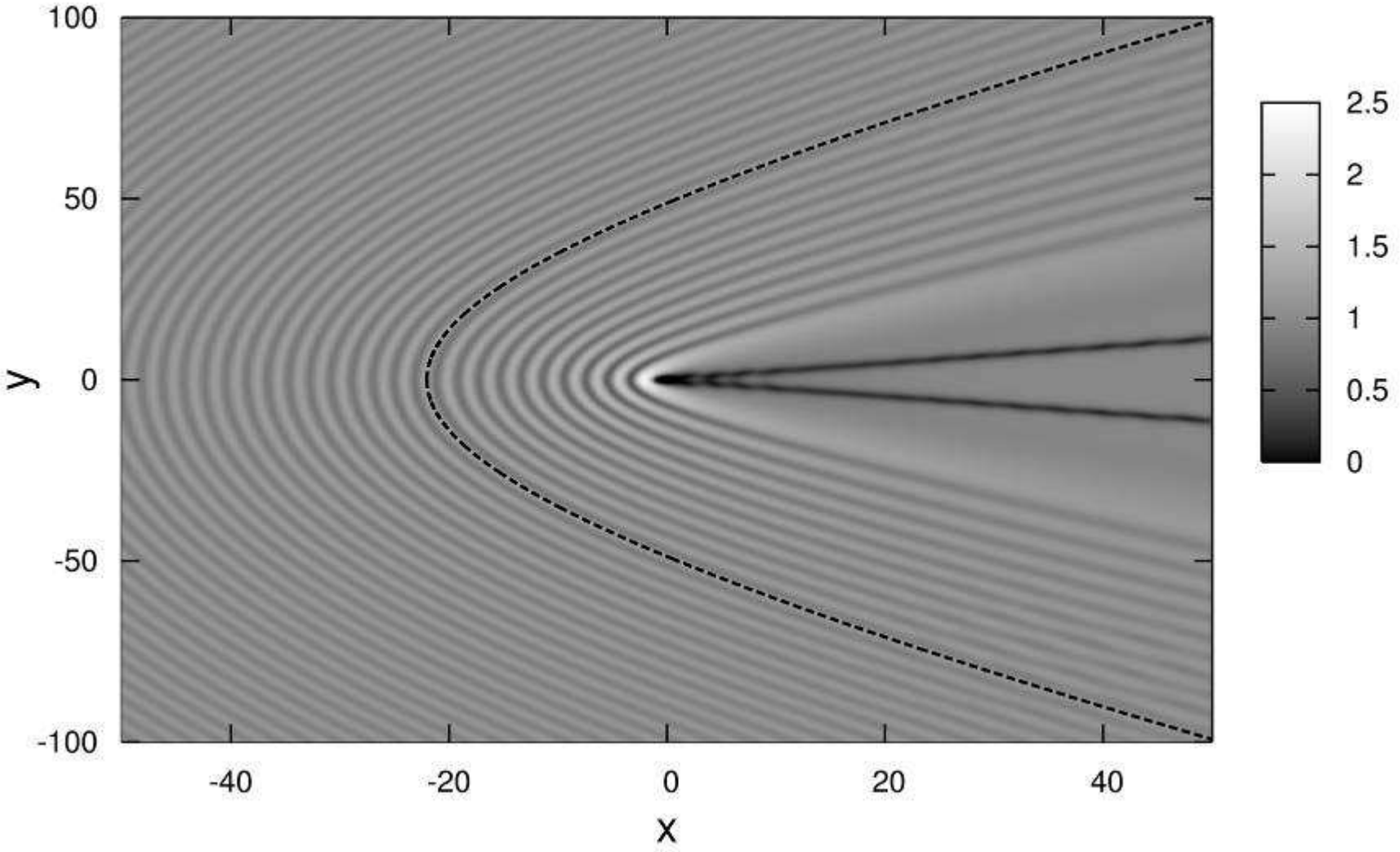

Yu.G. Gladush, G. El, A. G., A.M. Kamchatnov PRA (2007)

the source
ed in this
es emitted
by a strong
,7], to the
supersonic
[8], and in
by a boat
Letter we
erturbation
hich flows
perimental
a Galilean
e in a sta-
of a uni-
stationary
y letting a
localized

the BEC density profile after different expansion times t_{exp} are then taken by means of destructive absorption imaging. Two examples are shown in Fig. 1. The field of view is centered in the region around the defect in order to observe

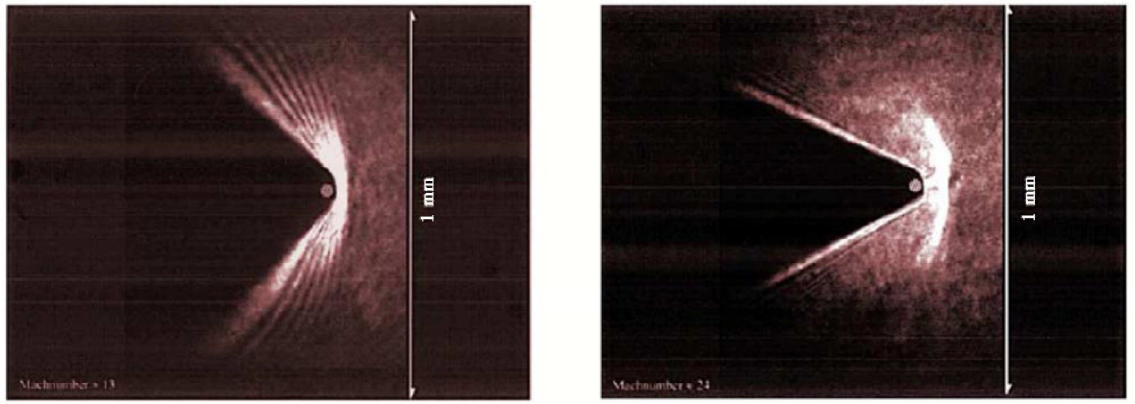

FIG. 1 (color online). Experimental [10] density profiles (integrated along z) of a BEC hitting an obstacle at supersonic velocities $v/c_s = 13$ (a) and 24 (b). The angles of the conical wave fronts are $\sin(\theta) = 0.73$ and $\sin(\theta) = 0.43$, respectively. The condensate flow is from the right to the left.

JILA

Carusotto et.al, PRL(2006)

Expansion in 2D, r=1

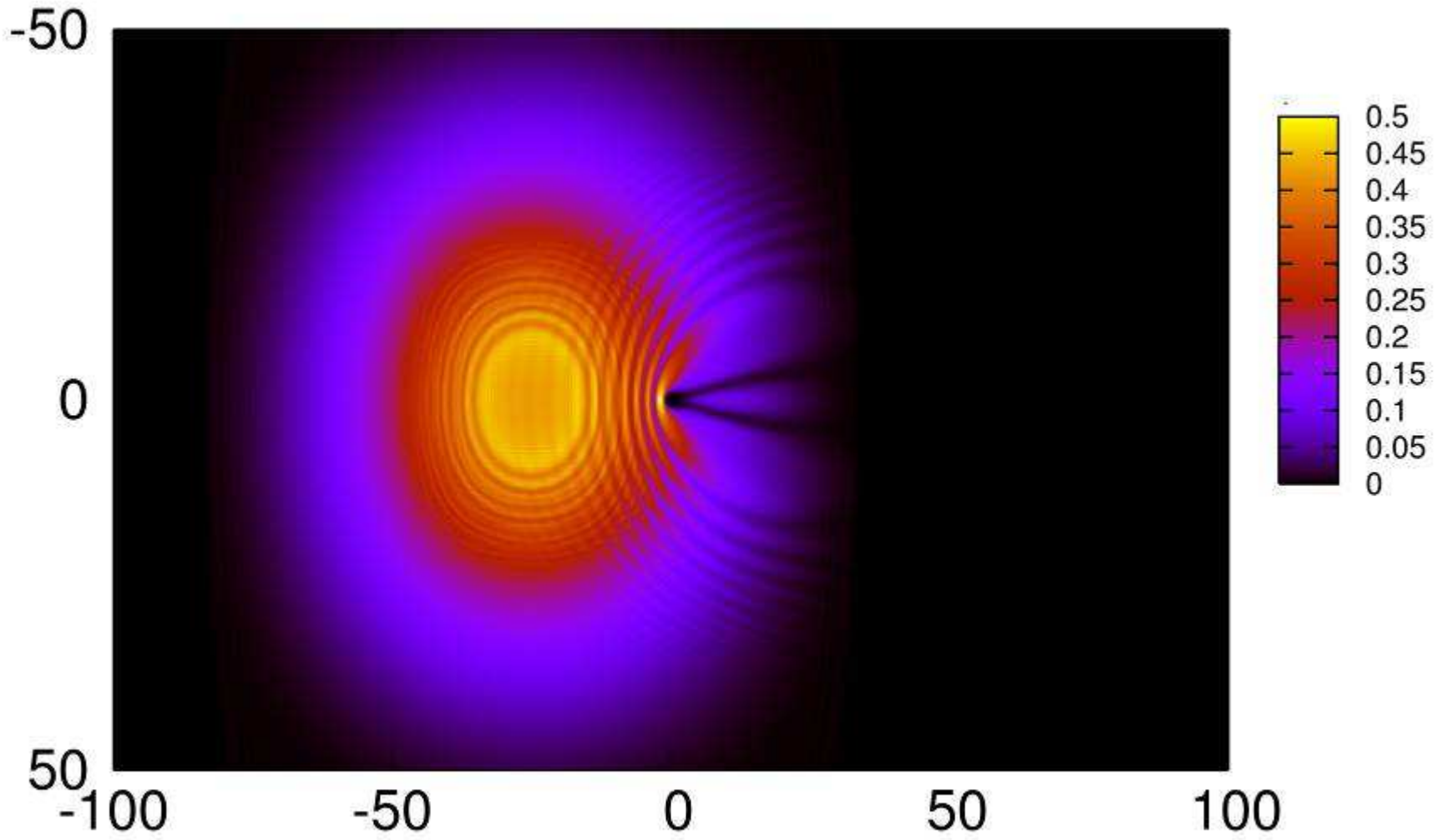

Thanks to referee…

Nonlinear optics “Hidrodynamics”

Within paraxial approximation luminous flow inside nonlinear Kerr medium (cristal) can be well described by

$$i\frac{\partial \psi}{\partial z} = -\frac{1}{2k_0}\nabla_{\perp}^2\psi - \frac{k_0}{n_0}\Delta n_2(|\psi|^2)\psi$$

where

$$\Delta n_2(|\psi|^2) = -\frac{1}{2}n_0^3 r_{33}E_p\frac{\rho}{\rho+\rho_d}, \qquad \rho = |\psi|^2$$

$\psi =$ *envelope field strength of EM wave*

n_0 = *linear refracting index*

E_p= *applied electric field*

r_{33}= *electro optical index*

$k_0 = 2\pi n_0/\lambda$ wave number

$\rho_d =$ saturation parameter

Gross-Pitaevskii 2D equation

$$i\hbar\frac{\partial\psi}{\partial t}=-\frac{\hbar^2}{2m}\Delta\psi+V_{ext}(\mathrm{r})\psi+g\,|\psi|^2\,\psi$$

Nonlinear optics 2D equation

$$i\frac{\partial\psi}{\partial z}=-\frac{1}{2k_0}\nabla_\perp^2\psi-\Delta n(|\psi|^2)\psi$$

different type of shock wave can emerge whose behaviour is dominated by dispersion rather than dissipation. Dispersive shock waves are difficult to study experimentally, and analytical solutions to the equations that govern them have only been found in one dimension (1D). By exploiting a well-known, but little appreciated, correspondence between the behaviour of superfluids and nonlinear optical materials, we demonstrate an all-optical experimental platform for studying the dynamics of dispersive shock waves. This enables us to observe the propagation and nonlinear response of dispersive shock waves, including the interaction of colliding shock waves, in 1D and 2D. Our system offers a versatile and more accessible means for exploring superfluid-like and related dispersive phenomena.

Unlike dissipative shock waves in ordinary gases/fluids, which have a well-defined shock front due to viscosity, dispersive superfluid-like shock waves have an oscillatory front. These oscillations result from two basic, and related, properties of the superfluid state: nonlinearity and coherence. Coherence results from cooling the fluid, so that the constituent particles of the condensate are perfectly correlated, whereas nonlinearity refers to the interparticle interactions that make this correlation possible. For different reasons, these two properties also occur in nonlinear optics. Although the relationship is well known in the condensate community (for example, nonlinear 'atom optics' studies in Bose–Einstein condensates (BEC)[1–3]), the relationship has been underappreciated from the opposite perspective. Here, we build on previous theoretical[4,5] and experimental[6,7] work on superfluid behaviour in BEC to examine the optical equivalent of condensate shock waves. We demonstrate basic dispersive, dissipationless shock waves in one and two transverse dimensions, characterize their nonlinear properties and reveal the non-trivial interactions when two such shocks collide.

Although dispersive shock waves in optics have been studied previously for temporal pulses in fibres[8–16], they have not yet been considered in the spatial domain. In this case, the extra dimensional freedom allows consideration of wavefront geometry, which is shown to significantly affect shock propagation and interaction. The particular system considered here is a spatial one in which a continuous optical wave propagates in a nonlinear Kerr-like medium, mainly along the z axis. To an excellent approximation, the slowly varying amplitude ψ of such a field can be described by the nonlinear Schrödinger equation:

$$i\frac{\partial\psi}{\partial z}+\frac{1}{2k_0}\nabla_\perp^2\psi+\Delta n(|\psi|^2)\psi=0 \qquad (1)$$

where $k_0=2\pi n_0/\lambda$ is the wavenumber, λ/n_0 is the wavelength in a homogeneous medium of refractive index n_0 and

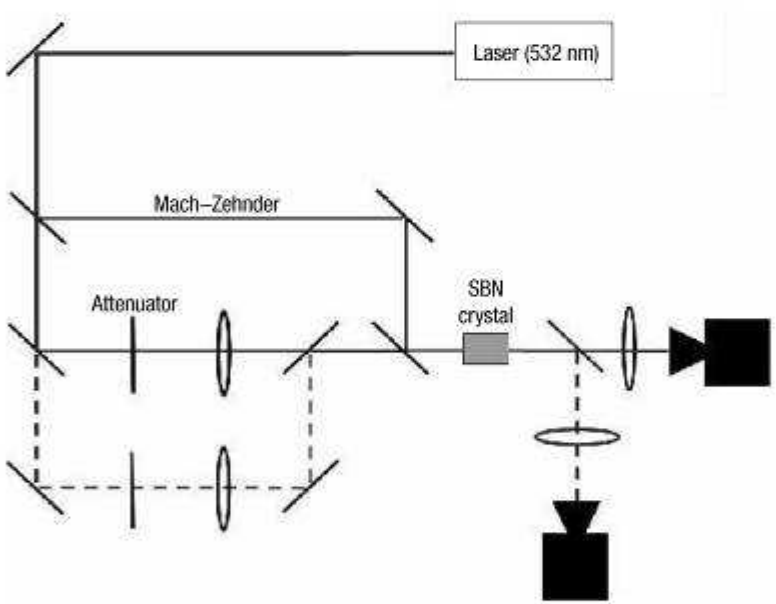

Figure 1 Experimental set-up. Light from a laser is split using a Mach–Zehnder interferometer. A cylindrical/circular lens placed in one of the arms focuses a beam onto the input face of an SBN:75 photorefractive crystal. For the nonlinear experiments, a constant voltage of −500 V is applied across the crystalline c axis to set the photorefractive screening effect, whereas the shock strength is controlled by varying the hump:background intensity ratio with an attenuator. Light exiting the crystal is then imaged into a charge-coupled-device camera. Both position (**x**) space and momentum (**k**) space are imaged. For the collision experiments, a second lensing arm in the interferometer is added.

W.Wan, S.Jia, J.W. Fleischer, Nature Physics (2006)

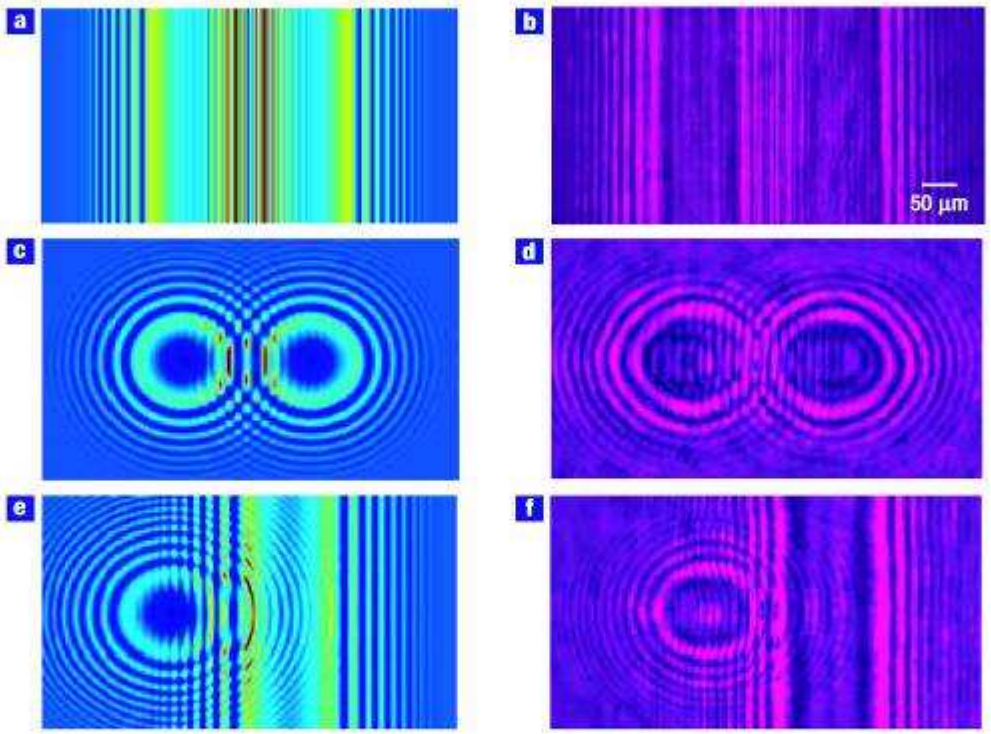

Figure 6 Shock wave collisions. Left column: Beam-propagation simulations. Right column: Experimental output pictures. **a**,**b**, 1D collision. **c**,**d**, 2D collision. **e**,**f**, 1D-on-2D shock collision. The outer regions show undisturbed shock behaviour, whereas the inner regions reveal the non-trivial interaction of nonlinear, dispersive waves. In particular, the wavefronts penetrating each circle in **c** and **d** are straight, the right-going wavefronts in **e** and **f** are flattened and the left-going wavefronts in **e** and **f** become concave.

therefore show individual profiles), whereas in Fig. 4b the initial condition is chosen so that the waves do not intersect in the linear case but do overlap in the nonlinear case. Despite the low intensity in the leading edges, the profile shows that shock collision is an inherently nonlinear process. As shown in Fig. 4b, the collision region has (1) a lower maximum intensity than the expected 4× gain of linear superposition, (2) an internal period of 7 μm, significantly more than the 5 μm expected from a linear sum of fronts are stable during propagation and do not generate vortices even after (head-on) collision. We conjecture that the array-like structure of the front is responsible for this, as individual 1D dark solitons suffer a snake instability (leading to vortices) in two transverse dimensions[46,47] but 1D arrays are stable[48,49].

Power spectra of 1D shock interactions, obtained by carrying out on optical Fourier transform on the output profiles in Fig. 4, are shown in Fig. 5. The linear reference case, that of two

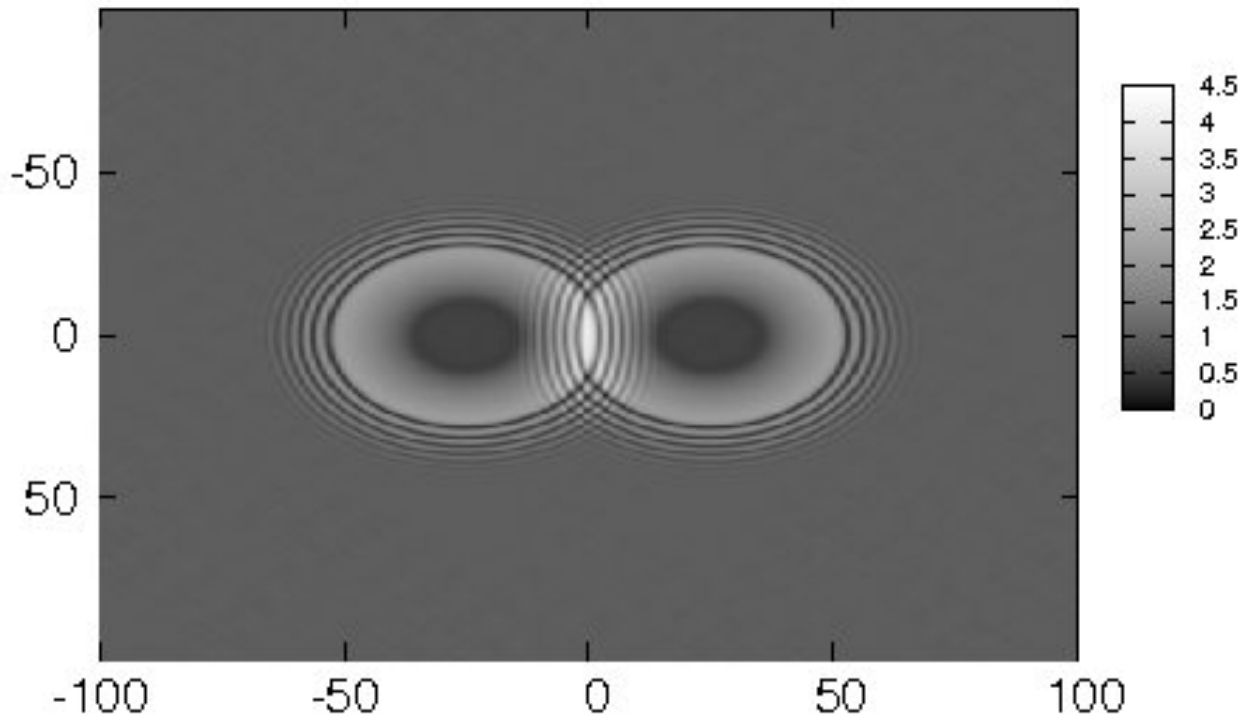

G.A.El, A.G., E.G.Khamis, R.A.Kraenkel, A.M.Kamchatnov PRA (2007).

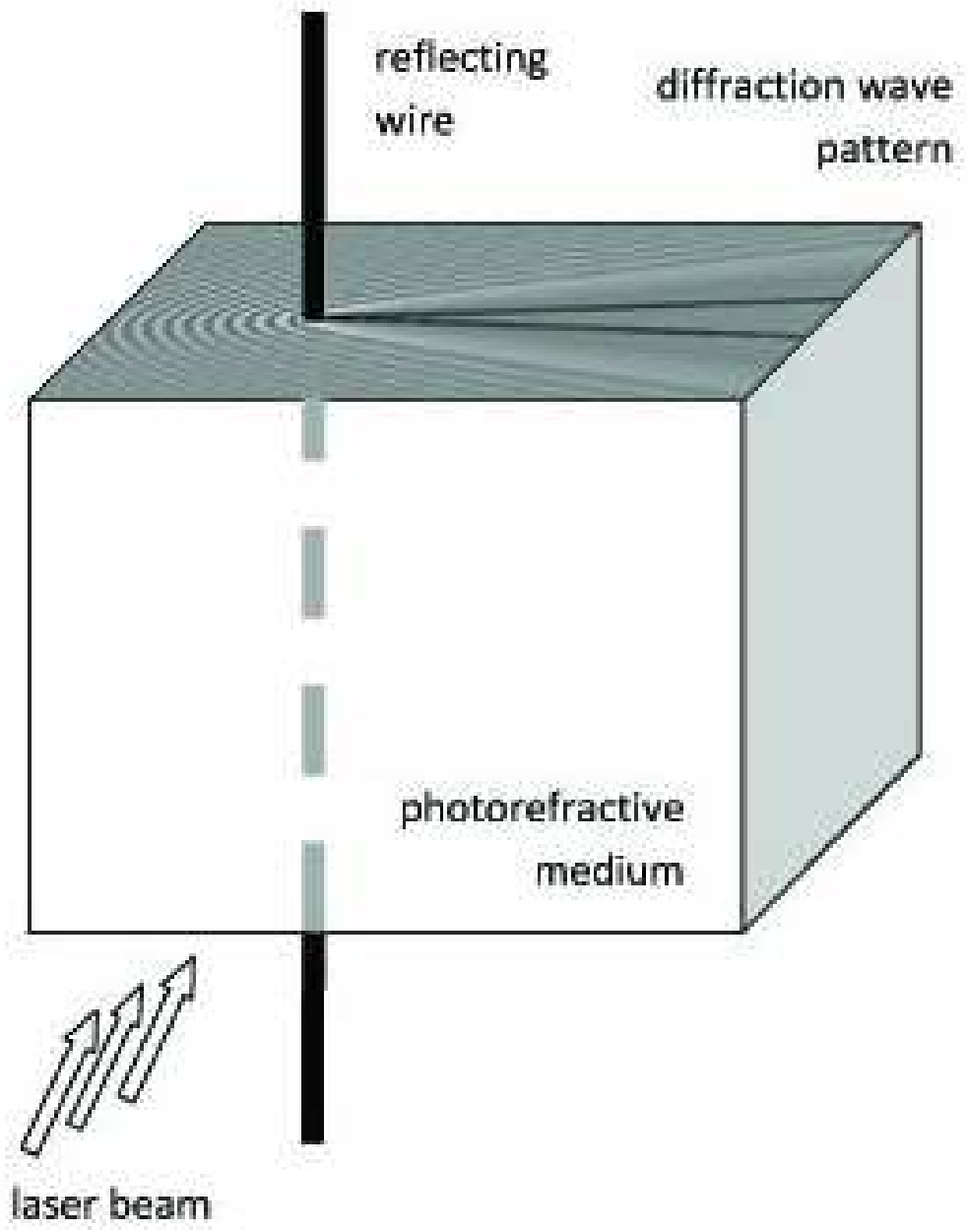
reflecting
wire
diffraction wave
pattern
photorefractive
medium
laser beam

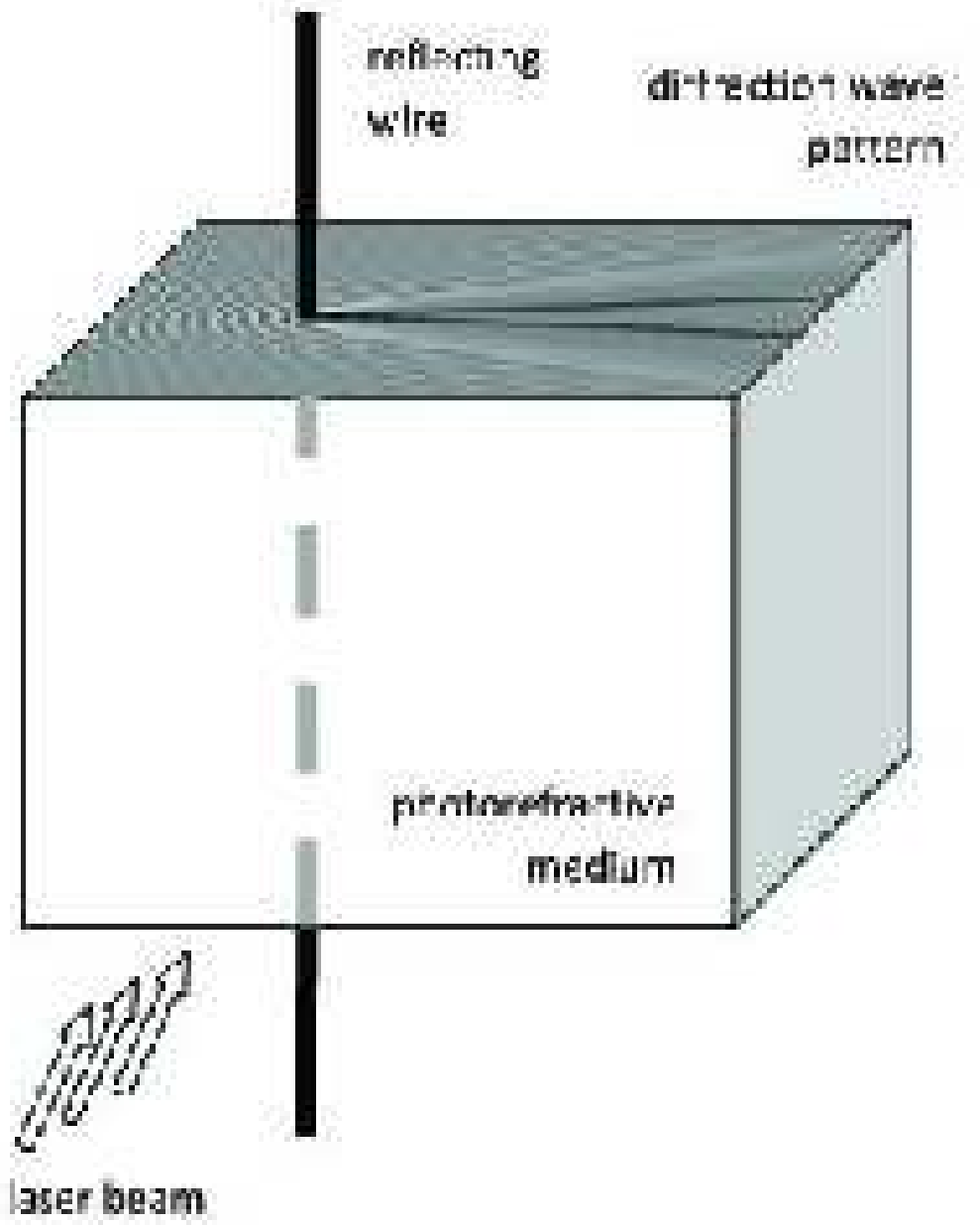
reflecting
wire
diffraction wave
pattern
photorefractive
medium
laser beam

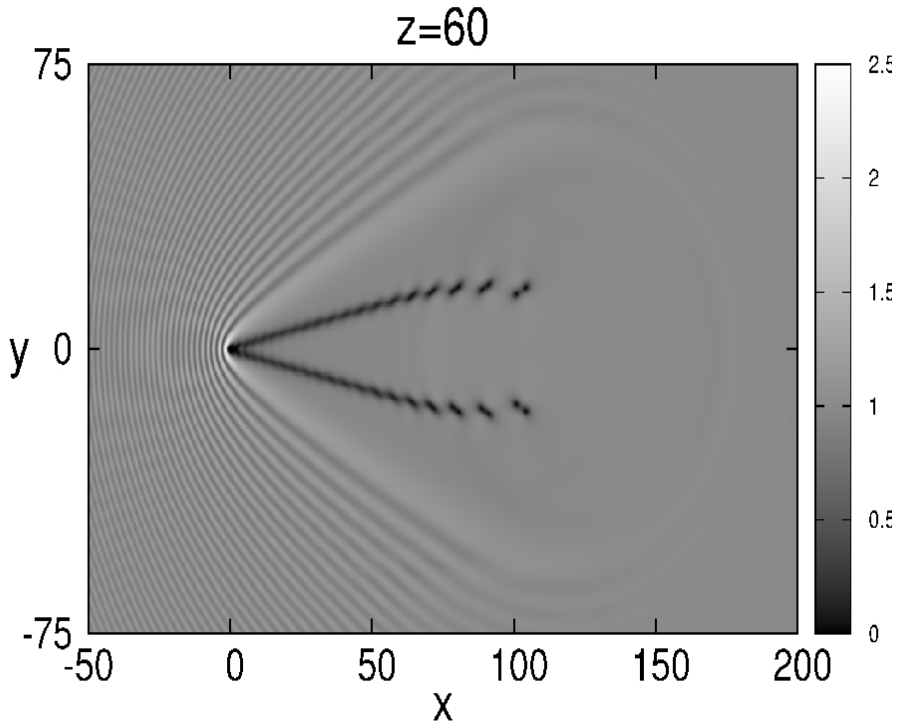

density

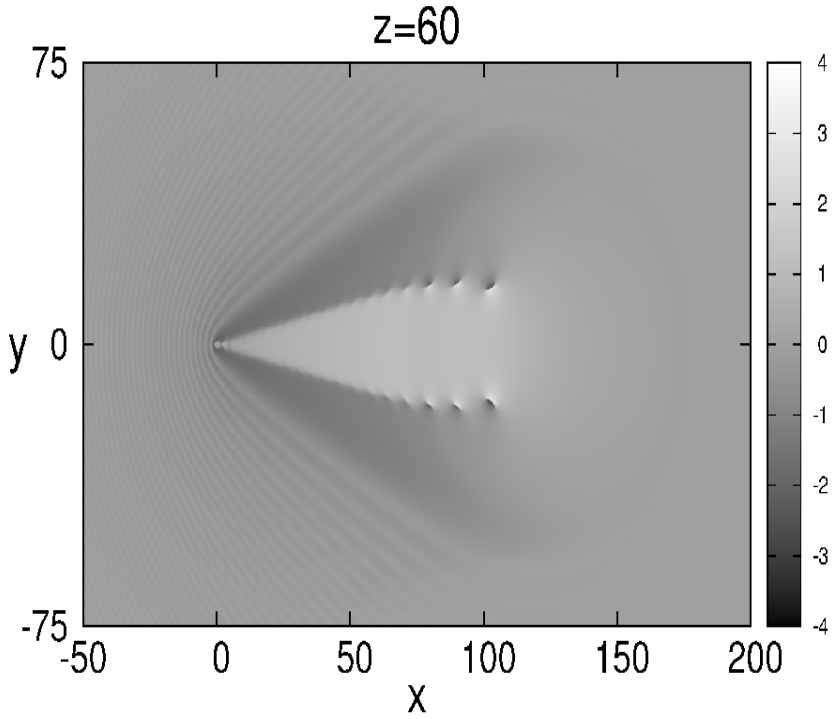

phase

Conclusions

-As we increase the velocity to supersonic velocities
the vortex generation turns to a ***continuum***

-This “vortex street” can be shown **analytically** and numerically
to be an oblique dark soliton. **REMARKABLE RESULT**

-Complex multi-soliton formations arise when we
increase the obstacle radius

-Hope that experimentalists in BEC and in Nonlinear crystals
can detect these dark solitons!

Outros projetos

-Dinâmica de condensados em redes
óticas não lineares
c/ Prof. F.Abdullaev (Uzbekistão)
estudantes : Hedhio Luz

-Condesados densos e
férmions ultrafrios (DAAD) c/
Prof. Klaus Ziegler (Alemanha)

To finish I recall someone that well understand Fluid Dynamics …


Thank You !

Sound in gas
de Bose
MIT (1997)